NIH Public Access
Author Manuscript
Invest Ophthalmol Vis Sci. Author manuscript; available in PMC 2010 February 1.

Published in final edited form as:
Invest Ophthalmol Vis Sci. 2009 February ; 50(2): 950–958. doi:10.1167/iovs.08-2544.

Rod and Rod-driven Function in Achromatopsia and Blue Cone Monochromatism

Anne Moskowitz, **Ronald M. Hansen**, **James D. Akula**, **Susan E. Eklund**, and **Anne B. Fulton**
Department of Ophthalmology, Children's Hospital and Harvard Medical School, 300 Longwood Avenue, Boston, MA 02115

Abstract

Purpose—To evaluate rod photoreceptor and postreceptor retinal function in pediatric patients with achromatopsia (ACHR) and blue cone monochromatism (BCM) using contemporary electroretinographic (ERG) procedures.

Methods—Fifteen patients (age 1 to 20 years) with ACHR and six patients (age 4 to 22 years) with BCM were studied. ERG responses to full-field stimuli were obtained in scotopic and photopic conditions. Rod photoreceptor (**S_{rod}**, **R_{rod}**) and rod-driven postreceptor (**log σ**, **V_{max}**) response parameters were calculated from the a-wave and b-wave. The ERG records were digitally filtered to demonstrate the oscillatory potentials (OPs); a sensitivity parameter, **log $SOPA_{1/2}$**, and an amplitude parameter, **$SOPA_{max}$**, were used to characterize the OP response. Response parameters were compared to those of 12 normal control subjects.

Results—As expected, photopic responses were non-detectable in patients with ACHR and BCM. In addition, mean scotopic photoreceptor (**R_{rod}**) and postreceptor (**V_{max}** and **$SOPA_{max}$**) amplitude parameters were significantly reduced compared to those in normal controls. The flash intensity required to evoke a half maximum b-wave amplitude (**log σ**) was significantly increased.

Conclusions—The results of this study provide evidence that deficits in rod and rod mediated function occur in the primary cone dysfunction syndromes, achromatopsia and blue cone monochromatism.

Achromatopsia refers to a group of congenital, stationary retinal disorders in which there is an absence or paucity of functioning cones.[1–3] Complete achromatopsia (ACHR), also called rod monochromatism, is an autosomal recessive condition characterized by reduced visual acuity, photophobia, nystagmus, deficits in color discrimination, and paradoxical pupillary constriction to dark.[1–5] Hyperopia is common [1, 6, 7], although a broad distribution of refractive errors has been reported.[8] Fundus appearance is typically normal [1–5], although exceptions have been reported.[9, 10] Blue cone monochromatism (BCM) is an X-linked condition that shares many of the characteristics of autosomal recessive achromatopsia, sometimes exhibited with reduced severity.[1–3, 11, 12] Refractive error, however, is typically myopic.[8, 11, 13–15] Clinically, the Berson plates discriminate patients with BCM from patients with ACHR.[16–18]

In ACHR, rods are the only functional photoreceptor type, while in BCM, both rods and short wavelength sensitive cones are functional.[12, 19] ACHR and BCM are typically regarded as

Corresponding author: Anne Moskowitz, Phone: 617-355-5122, Fax: 617-730-0392, e-mail: Anne.Moskowitz@childrens.harvard.edu.

Presented in part at the annual meeting of the Association for Research in Vision and Ophthalmology, Fort Lauderdale, Florida, May 2007.

Disclosure: A. Moskowitz, None; R. M. Hansen, None; J. D. Akula, None; S. E. Eklund, None; A. B. Fulton, None.

NIH-PA Author Manuscript
NIH-PA Author Manuscript
NIH-PA Author Manuscript

NIH-PA Author Manuscript

NIH-PA Author Manuscript

NIH-PA Author Manuscript

stationary conditions, but in both there have been reports of adults with progressive retinal disease.[10, 20–26]

Achromatopsia is understood to be a channelopathy of the cone photoreceptors. The most common molecular causes are mutations in the cGMP-gated cation channel genes *CNGA3* (OMIM600053) and *CNGB3* (OMIM605080).[7, 27–31] Less frequently, a mutation in the transducin protein *GNAT2* (OMIM139340) has been associated with achromatopsia.[32, 33] The most common molecular causes of BCM are mutations in the opsin gene array of long and medium wavelength sensitive cone visual pigments located adjacently on the X-chromosome. (OMIM303700).[25, 34]

In both ACHR and BCM, cone and cone-driven electroretinogram (ERG) responses to full-field stimuli are markedly attenuated or non-detectable, whereas rod and rod-driven responses are typically reported to be normal or near normal.[4, 6, 8, 9, 21, 26, 27, 35–40] Recently, however, abnormal rod-driven ERGs have been reported in some patients with *CNGB3* achromatopsia [10] and BCM.[23]

Our own clinical observations also indicated abnormalities in rod and rod-driven ERGs in pediatric patients with achromatopsia and blue cone monochromatism. Therefore, we undertook an analysis of rod photoreceptor and postreceptor ERG components. Our goal was to identify possible mechanisms underlying the abnormalities.

Methods

Subjects

Twenty one patients (Table 1), 15 with complete achromatopsia (ACHR) and six with blue cone monochromatism (BCM), who had been followed in the Department of Ophthalmology, Children's Hospital Boston were studied retrospectively. ACHR patients exhibited typical features of achromatopsia, including low visual acuity; photophobia; low amplitude, high frequency, "jelly-like" nystagmus; and paradoxical pupillary constriction to dark. All patients had normal fundus appearance. ACHR patients #1 and #8 are siblings. The clinical presentation of the patients with BCM was similar, although the photophobia often appeared less severe. All were male and all passed the Berson test;[16] that is, unlike patients with ACRH, they were able to distinguish a purple-blue (Munsell Color System 7.5 PB; dominant wavelength 468 nm) arrow from blue-green (5.0 BG; 491 nm) arrows. Two males who were classified as ACHR (ACHR #4 and #7) were too young to do color vision testing. Median age at ERG was 2.7 years (range 1 to 20 years) for the ACHR patients and 8.0 years (range 4 to 22 years) for the BCM patients.

Visual acuity was measured in dim room light using age appropriate tests (Teller Acuity Cards, HOTV, Lea, Feinbloom, or ETDRS). Refractive error was measured using cycloplegic retinoscopy.[41] The most recent visual acuity and spherical equivalent values for each patient are reported in Table 1. Acuity was below normal for age in all patients. Twelve of the 15 ACHR patients were hyperopic; nine were outside the 99% prediction limit of normal for age.[41, 42] Two of the three myopic ACHRs were also outside the normal limit. All six BCM patients were myopic; four were outside the 99% prediction limit of normal for age.

Dark adapted, rod mediated visual thresholds, obtained in 11 ACHR patients and five BCM patients, were normal [43] in all but one (ACHR #7), who showed a mild (1.18 log units) but statistically significant threshold elevation. Four patients had repeated measurements with a 1.5 year (ACHR #5), a 6.8 year (BCM #21), a 7.8 year (ACHR #9), and a 9.0 year (ACHR #12) interval between tests, and none showed a change in threshold, suggesting a stationary condition.

NIH-PA Author Manuscript

NIH-PA Author Manuscript

NIH-PA Author Manuscript

ERG responses in the patients with ACHR and BCM were compared to responses in 12 healthy control subjects (median age 23 years; range 8 to 41 years). ERG response parameters in normal subjects at the ages of our patients with ACHR and BCM (1 to 22 years) do not differ significantly from those in adults.[44] All of the control subjects had normal ocular structures and corrected visual acuity of 20/25 or better; median spherical equivalent was −0.50 D (range −4.75 to +0.88 D).

The patients had been referred for examination and testing in an attempt to diagnose their eye and vision problems. Analysis of the patients' data was done retrospectively with the approval of the Children's Hospital Committee on Clinical Investigation (CCI). Written, informed consent was obtained from the control subjects after explanation of the nature and possible consequences of the study. The control study conformed to the tenets of the Declaration of Helsinki and was approved by the Children's Hospital CCI.

Electroretinography

Pupils were dilated with 1% cyclopentolate hydrochloride, and the patient was dark adapted for 30 minutes. All 12 control subjects and seven patients (four ACHR, three BCM) were tested awake (Table 1); fifteen patients (11 ACHR, three BCM) had ERG testing under light inhalation anesthesia which has no significant effect on the ERG parameters studied herein.[45] Following dark adaptation, 0.5% proparacaine was instilled and, under dim red light, a bipolar Burian-Allen electrode (Hansen Ophthalmic Development Laboratory, Coralville, IA) was placed on the cornea. A ground electrode was placed on the skin over the mastoid. Responses were recorded from both eyes of the patients and from one eye of the control subjects. In patients, the eye with the larger scotopic amplitudes was selected for analysis.

Thirteen of the patients (10 ACHR, three BCM) and all 12 control subjects were tested using a Compact 4 system (Nicolet, Madison, WI) and eight (five ACHR, three BCM) using an Espion system (Diagnosys, Lowell, MA). Despite differences between the two recording systems in the spectral composition of the stimuli (described below) and in data acquisition (2,564 Hz digitization rate for the Nicolet; 2,000 Hz for the Espion), a previous comparison[46] of rod and cone photoresponse parameters in normal adult subjects obtained using the Espion system (N=7) and obtained earlier using the Nicolet system (N=13) [44, 47] showed no significant differences. Therefore, the data obtained using the two systems have been combined.

Responses were differentially amplified, displayed, digitized, and stored for analysis. A voltage window was used to reject responses contaminated by artifacts. Two to 16 responses were averaged in each stimulus condition. The inter-stimulus interval ranged from 2 to 60 seconds and was selected so that subsequent b-wave amplitudes were not attenuated.[47]

Full-field stimuli were presented in an integrating sphere. Stimulus intensity was measured using a calibrated photodiode (IL1700; International Light, Newburyport, MA) placed at the position of the subject's cornea. The troland values of the stimuli were calculated by taking each subject's pupillary diameter into account. To test rod function, after dark adaptation, responses to brief (<3 ms), short wavelength stimuli ranging from those that evoked a small b-wave (<15 μVolts) to those saturating the a-wave were recorded. In the Nicolet system, a Wratten 47B filter (λ<510 nm) was used; in the Espion system, a 470 nm LED (half bandwidth 30 nm) was used. Flashes were presented over a >4 log unit range, starting with the dimmest and increasing in 0.3 log unit steps. The maximum intensity flash produced approximately 3.0 log scotopic troland seconds (scot td sec) for an 8 mm pupil.

NIH-PA Author Manuscript

NIH-PA Author Manuscript

NIH-PA Author Manuscript

To isolate rod function in the control subjects, dark adapted responses to photopically matched long wavelength flashes (Wratten 29 filter, λ>610 nm) were recorded and subtracted from the responses to the corresponding short wavelength flashes.[48]

Cone function was tested using long wavelength flashes. In the Nicolet system, a Wratten 29 filter (λ >610 nm) was used; in the Espion system, a 630 nm LED (half bandwidth 30 nm) was used. A 1.8 log unit range of red flash intensities was presented on a steady, rod-saturating background (~3 log phot td). The maximum intensity flash produced approximately 3.2 log photopic troland seconds (phot td sec) for an 8 mm pupil. Seventeen of the 21 patients were also tested with a 30 Hz flickering white stimulus (2.4 log phot td sec).

The rod photoresponse characteristics were estimated from the a-wave by means of the Hood and Birch formulation [49] of the Lamb and Pugh model [50–52] of the biochemical processes involved in the activation of rod phototransduction. A curve fitting routine (MATLAB, fmins subroutine; The MathWorks, Inc, Natick, MA) was used to determine the best fitting values of $\mathbf{S_{rod}}$ [(scot td)$^{-1}$ sec^{-3}], $\mathbf{R_{rod}}$ (μVolts), and $\mathbf{t_d}$ (a brief delay, sec) in the following equation:

$$P3(I,t)=\{1-\exp[-0.5\,I\,\mathbf{S_{rod}}(t-\mathbf{t_d})^2]\}\mathbf{R_{rod}} \quad \text{for } t>\mathbf{t_d} \qquad \text{Eq. 1}$$

In this equation, I is the flash in scotopic troland seconds. Assuming that the number of isomerizations of rhodopsin produced by the stimulus is known, the term $\mathbf{S_{rod}}$ is related to the amplification constant, **A**, in the molecular models.[50–53] In these models, **A** summarizes the kinetics of the series of processes, initiated by the photoisomerization of rhodopsin, that result in closure of the channels in the plasma membrane of the photoreceptor. $\mathbf{R_{rod}}$ is an estimate of the amplitude of the saturated response. Fitting of the model was restricted to the leading edge of the a-wave or to a maximum of 20 ms after stimulus onset.

The b-wave responses to short wavelength flashes were also analyzed. The stimulus/response function

$$V(I)=\mathbf{V_{max}}[I/(I+\sigma)] \qquad \text{Eq. 2}$$

was fit to the b-wave amplitudes of each subject. In this equation, V is the b-wave amplitude produced by flash intensity I, $\mathbf{V_{max}}$ (μVolts) the saturated amplitude, I the stimulus in scot td sec, and σ the stimulus that evokes a half-maximum b-wave amplitude. The function was fit only up to those higher intensities at which substantial a-wave intrusion occurred (~+1.0 log scot td sec).[54]

As established by Granit, the ERG waveform represents the algebraic sum of photoreceptor and postreceptor retinal responses.[55, 56] The isolated rod photoresponse, called P_3, is modeled by Equation 1. To evaluate postreceptor function, designated P_2, a putatively “pure” postreceptor response was isolated from the intact ERG by digital subtraction of P_3 from the record. P_2 represents primarily the bipolar cell response.[57–61]

For P_2, the relation between flash intensity and the elapsed time between stimulus presentation and the instant at which the response reaches an arbitrary criterion voltage will be linear on a log-log plot with slope −0.2 in normal retina, consistent with three stages of integration in the rod photoreceptor and three stages of integration in the rod bipolar cell.[59] Departures from this relation indicate dysfunction of the ON bipolar cells’ G-protein cascade.[59, 60] We selected a 50 μVolt criterion and noted the latency at which the rising phase of P_2 reached that criterion. For a family of P_2 waves, we plotted the latency versus intensity relationship. To test for

NIH-PA Author Manuscript

NIH-PA Author Manuscript

NIH-PA Author Manuscript

dysfunction, regression lines were fit and the slope of the regression line (**P_2 slope**) in patients was compared to that in control subjects.

Oscillatory potentials (OPs) were extracted from the derived postreceptor response (P_2) as described previously.[62] In brief, P_2 was digitally filtered using a fifth-order Butterworth filter (MATLAB; butter subroutine; The MathWorks, Inc, Natick, MA) with bandpass 75 to 300 Hz.[63] The amplitude (μV) of each OP wavelet was defined as the difference between the peak and the trough immediately preceding it. To characterize the OPs, the summed amplitude of the OPs (**SOPA**) at each intensity was plotted as a function of stimulus energy and the Michaelis-Menton equation

$$\mathrm{SOPA}(I)=\mathbf{SOPA_{max}}[I^n/(I^n+\mathbf{SOPA}_{1/2}{}^n)] \quad \text{Eq. 3}$$

was fit to the data. In this equation, SOPA(I) is the summed amplitude (μV) of the OPs in the response to a flash of I intensity, $\mathbf{SOPA_{max}}$ is the saturated amplitude (μV) of the OPs, and $\mathbf{SOPA_{½}}$ is the intensity at which the summed amplitude of the OPs is half $\mathbf{SOPA_{max}}$.

Statistical Analyses

Preliminary analyses showed no significant difference between ACHR and BCM patients on any of the ERG parameters ($\mathbf{S_{rod}}$, $\mathbf{R_{rod}}$, **log σ**, $\mathbf{V_{max}}$, **log** $\mathbf{SOPA_{1/2}}$, $\mathbf{SOPA_{max}}$, and **P_2 slope**; t-tests: df=19; P >0.2 on all tests). Furthermore, for each parameter, the range of values for ACHR and BCM patients was similar. Therefore, data from the two patient groups were pooled and individual, independent samples t-tests for each ERG parameter were used to detect differences between patients and control subjects. The significance level for all tests was $P<0.01$.

Results

In Figure 1, sample ERG records from an ACHR patient obtained in scotopic (Fig. 1A) and photopic (Fig. 1B) conditions are shown. In all patients with ACHR or BCM, scotopic activity was observed over a ≥3 log unit range of intensities, while photopic activity was absent or markedly attenuated (<5% of normal mean amplitude). Figure 1C shows sample fits of the model (Eq. 1) of the activation of rod phototransduction [49–52] to the a-wave. Figure 1D shows the fit of Eq. 2 for determining the postreceptor (b-wave) response parameters. Note that lower values of **log σ** indicate greater sensitivity; that is, a lower intensity produces the half maximum response.

Figure 2 shows P_2 responses derived from the records in Figure 1A and a plot of the latency versus intensity relationship. Scotopic OP records extracted from the P_2 responses shown in Figure 2 are displayed in Figure 3; OPs from a control subject are also shown.

The rod photoreceptor and postreceptor response parameters for the patients with ACHR and BCM and for control subjects are summarized in Figure 4. The amplitude parameters for the rods, $\mathbf{R_{rod}}$ ($t = -7.484$, df=31, $P<0.001$), and for postreceptor activity, $\mathbf{V_{max}}$ ($t = -6.821$, df=31, $P<0.001$) and $\mathbf{SOPA_{max}}$ ($t = -10.755$, df=31, $P<0.001$), were significantly lower in patients than in controls, with little overlap. For all sensitivity parameters ($\mathbf{S_{rod}}$, **log σ**, and **log** $\mathbf{SOPA_{1/2}}$), there was substantial overlap between patients and controls. However, b-wave **log σ** in patients differed significantly from that in controls ($t = 3.152$, df = 31, $P = 0.0036$); in patients, a higher intensity was needed to evoke a half maximum response. In prior study of young, healthy subjects with myopia (as high as −10 diopters), we found no differences in rod and rod-driven postreceptor response parameters between myopes and controls.[64]

NIH-PA Author Manuscript

NIH-PA Author Manuscript

NIH-PA Author Manuscript

The mean slope of regression lines fit to P_2 latency versus intensity plots was −0.19 (SD=0.04) in the 12 control subjects and −0.20 (SD = 0.04) in the ACHR and BCM patients. These values were not significantly different from each other or from the normal mean slope of −0.2.[59, 60, 65]

Discussion

In these young patients with achromatopsia (ACHR) and blue cone monochromatism (BCM), we have demonstrated significant deficits in rod and rod-driven function. Specifically, mean photoreceptor ($\mathbf{R_{rod}}$) and postreceptor ($\mathbf{V_{max}}$ and $\mathbf{SOPA_{max}}$) amplitude parameters were reduced relative to those in normal controls (Figure 4). Sensitivity parameters ($\mathbf{S_{rod}}$, **log σ**, and $\mathbf{log\ SOPA_{1/2}}$) were less affected; only b-wave **log σ** differed significantly from normal.

While rod photoreceptors are not directly affected by the genetic mutations causing ACHR and BCM, it has been suggested that alterations in rod structure occur. High resolution adaptive optics imaging of the photoreceptor mosaic in a subject with *CNGB3* achromatopsia showed increased diameter of rod inner segments, possibly due to rods expanding into space that would normally be occupied by cones.[66] In this subject, the density of rods at 10° eccentricity was reduced by about a third compared to normal.[66, 67] Thus, the low values of $\mathbf{R_{rod}}$ in our ACHR and BCM subjects may be due to a decrease in the total number of rods. Shorter rod outer segment length would also reduce $\mathbf{R_{rod}}$. To our knowledge, rod outer segment length has not been measured in ACHR or BCM.

To our knowledge, only one other study [10] quantitatively investigated rod activation in patients with ACHR. Khan and colleagues evaluated four adults with *CNGB3* achromatopsia who showed macular atrophy in middle age. Their rod photoreceptor and postreceptor amplitude parameters fell within the range of values observed in our patients. Our patients, however, were younger than theirs (Table 1) yet the majority showed greater deficits. We have observed neither fundus abnormalities nor progressive worsening in visual acuity or dark adapted visual thresholds in our patients. We wonder, therefore, if the alterations in rod and rod-driven function may indicate anomalies in rod pathway signaling rather than rod disease. Individuals with ACHR and BCM prefer dim environments, which would increase the metabolic load placed on the rods. This, in turn, would result in more circulating current, which would require more energy with possible adverse long term effects on rod function.

Thus, the low calculated values of $\mathbf{R_{rod}}$ could be due to fewer rods, shorter rod outer segments, or defective rod functioning.

In addition to the significant deficit in rod photoresponse amplitude, we observed deficits in postreceptor response parameters ($\mathbf{V_{max}}$, **log σ**, and $\mathbf{SOPA_{max}}$). According to an explicit model, changes in $\mathbf{R_{rod}}$ are predicted to alter b-wave sensitivity (**log σ**) but to have little effect on $\mathbf{V_{max}}$.[58, 68] In our patients, mean **log σ** and mean $\mathbf{V_{max}}$ are both approximately half that in controls. The low $\mathbf{V_{max}}$ could be caused by too few rod-driven bipolar cells. Although we are unaware of any anatomic evidence that the number of rod bipolar cells is reduced in ACHR or BCM, the reduced rod density found in the subject with achromatopsia [66] may be accompanied by a proportionate reduction in rod bipolar cell density. In another system (immature simian central retina), the numbers of cones and cone bipolar cells are proportionately decreased.[69] Another possible explanation for the reduction in $\mathbf{V_{max}}$ that is consistent with the explicit model [58, 68] is a postreceptor change resulting from abnormal function of rod bipolar cells. However, the normal P_2 latency versus intensity slope (Figure 2) indicates that, at the least, the G-protein amplification cascade in the rod bipolar cell was operational.

NIH-PA Author Manuscript

NIH-PA Author Manuscript

NIH-PA Author Manuscript

Our data do not allow us to exclude the possibility that there is some alteration of the rod-driven circuitry in ACHR and BCM. Reorganization of the postreceptor retina is a well documented consequence in a number of photoreceptor disorders.[62, 70–73] The normal scotopic pathway is dominated by the rod-specific hyperpolarizing bipolar cell.[74] In addition to this primary pathway, there are anatomical connections between rods and cones and some between rods and depolarizing cone bipolar cells.[75–81] We speculate that the latter contacts may be more numerous in cone-deficient ACHR and BCM retinas. This would allow substantial rod input to cone depolarizing bipolar cells with consequent reduction in the apparent postreceptor response from the primary rod pathway in both ACHR and BCM. In a CNGA3$^{-/-}$ mouse model, anomalous synapses between rods and cone bipolar cells are documented.[82]

The oscillatory potentials are affected by inputs from both rods and cones.[83, 84] In ACHR and BCM retinas, cone input is absent or greatly diminished, possibly accounting for the dramatic attenuation in **SOPA$_{max}$** observed in our patients.

Whatever the actual mechanisms, the ERG data reported herein add evidence that deficits in rod and rod mediated function occur in the primary cone dysfunction syndromes, achromatopsia and blue cone monochromatism. While it is well established that cones are adversely affected in primary rod disorders,[82, 85–91] there has been less evidence that rods are affected in disorders with primary cone dysfunction.[10, 23, 92]

Each of the possible mechanisms for abnormal retinal function considered above leads to hypotheses that can be tested by further ultra-high resolution imaging of individuals with ACHR and BCM and by study of animal models.[82, 92–94] The new knowledge obtained will bolster efforts to design and evaluate effective therapies for cone dysfunction syndromes.[95, 96]

Acknowledgements

Supported in part by National Eye Institute Grant EY 10597.

References

1. Michaelides, M.; Holder, G.; Moore, A. Inherited retinal dystrophies. In: Taylor, D.; Hoyt, C., editors. Pediatric Ophthalmology and Strabismus. 3. New York: Elsevier Saunders; 2005. p. 183-241.
2. Michaelides M, Hunt DM, Moore AT. The cone dysfunction syndromes. Br J Ophthalmol 2004;88:291–7. [PubMed: 14736794]
3. Pokorny, J.; Smith, VC.; Verriest, G. Congenital color defects. In: Pokorny, J.; Smith, V.; Verriest, G.; Pinckers, A., editors. Congenital and Acquired Color Vision Deficits. New York: Grune & Stratton; 1979.
4. Krill, AE. Congenital color vision defects. In: Krill, AE., editor. Hereditary Retinal and Choroidal Disease. 11. London: Harper & Row; 1977. p. 335-90.
5. Hansen, E. Clinical aspects of achromatopsia. In: Hess, R.; Sharpe, L.; Nordby, K., editors. Night Vision: Basic, Clinical and Applied Aspects. Cambridge: Cambridge University Press; 1990. p. 316-334.
6. Kelly JP, Crognale MA, Weiss AH. ERGs, cone-isolating VEPs and analytical techniques in children with cone dysfunction syndromes. Doc Ophthalmol 2003;106:289–304. [PubMed: 12737507]
7. Wissinger B, Gamer D, Jagle H, et al. CNGA3 mutations in hereditary cone photoreceptor disorders. Am J Hum Genet 2001;69:722–37. [PubMed: 11536077]
8. Haegerstrom-Portnoy G, Schneck ME, Verdon WA, Hewlett SE. Clinical vision characteristics of the congenital achromatopsias. I Visual acuity, refractive error, and binocular status. Optom Vis Sci 1996;73:446–56. [PubMed: 8843124]
9. Goodman G, Ripps H, Siegel IM. Cone dysfunction syndromes. Arch Ophthalmol 1963;70:214–31. [PubMed: 14060101]

NIH-PA Author Manuscript

NIH-PA Author Manuscript

NIH-PA Author Manuscript

10. Khan NW, Wissinger B, Kohl S, Sieving PA. CNGB3 achromatopsia with progressive loss of residual cone function and impaired rod-mediated function. Invest Ophthalmol Vis Sci 2007;48:3864–71. [PubMed: 17652762]
11. Spivey BE. The X-linked recessive inheritance of atypical monochromatism. Arch Ophthalmol 1965;74:327–33. [PubMed: 14338644]
12. Blackwell H, Blackwell O. Rod and cone receptor mechanisms in typical and atypical congenital achromatopsia. Vision Res 1961;1:62–107.
13. Francois J, Verriest G, Matton-Van Leuven T, De Rouck A, Manavian D. Atypical achromatopia of sex-linked recessive inheritance. Am J Ophthalmol 1966;61:1101–8. [PubMed: 5296062]
14. Weleber, R.; Eisner, A. Cone degeneration ('bull's eye dystropies') and colour vision defects. In: Newsome, D., editor. Retinal Dystropies and Degenerations. New York: Raven Press; 1988. p. 223-56.
15. Weiss AH, Biersdorf WR. Blue cone monochromatism. J Pediatr Ophthalmol Strabismus 1989;26:218–23. [PubMed: 2795409]
16. Berson EL, Sandberg MA, Rosner B, Sullivan PL. Color plates to help identify patients with blue cone monochromatism. Am J Ophthalmol 1983;95:741–7. [PubMed: 6602551]
17. Pinckers A. Berson test for blue cone monochromatism. Int Ophthalmol 1992;16:185–186. [PubMed: 1452423]
18. Haegerstrom-Portnoy G, Schneck ME, Verdon WA, Hewlett SE. Clinical vision characteristics of the congenital achromatopsias. II Color vision. Optom Vis Sci 1996;73:457–65. [PubMed: 8843125]
19. Sharpe, L.; Nordby, K. The photoreceptors in the achromat. In: Hess, R.; Sharpe, L.; Nordby, K., editors. Night Vision: basic, clinical and applied aspects. Cambridge: Cambridge University Press; 1990. p. 335-389.
20. Ayyagari R, Kakuk LE, Bingham EL, et al. Spectrum of color gene deletions and phenotype in patients with blue cone monochromacy. Hum Genet 2000;107:75–82. [PubMed: 10982039]
21. Ayyagari R, Kakuk LE, Coats CL, et al. Bilateral macular atrophy in blue cone monochromacy (BCM) with loss of the locus control region (LCR) and part of the red pigment gene. Mol Vis 1999;5:13. [PubMed: 10427103]
22. Fleischman JA, O'Donnell FE Jr. Congenital X-linked incomplete achromatopsia. Evidence for slow progression, carrier fundus findings, and possible genetic linkage with glucose-6-phosphate dehydrogenase locus. Arch Ophthalmol 1981;99:468–72. [PubMed: 6971088]
23. Kellner U, Wissinger B, Tippmann S, Kohl S, Kraus H, Foerster MH. Blue cone monochromatism: clinical findings in patients with mutations in the red/green opsin gene cluster. Graefes Arch Clin Exp Ophthalmol 2004;242:729–35. [PubMed: 15069569]
24. Michaelides M, Johnson S, Simunovic MP, et al. Blue cone monochromatism: a phenotype and genotype assessment with evidence of progressive loss of cone function in older individuals. Eye 2005;19:2–10. [PubMed: 15094734]
25. Nathans J, Davenport CM, Maumenee IH, et al. Molecular genetics of human blue cone monochromacy. Science 1989;245:831–8. [PubMed: 2788922]
26. Eksandh L, Kohl S, Wissinger B. Clinical features of achromatopsia in Swedish patients with defined genotypes. Ophthalmic Genet 2002;23:109–20. [PubMed: 12187429]
27. Nishiguchi KM, Sandberg MA, Gorji N, Berson EL, Dryja TP. Cone cGMP-gated channel mutations and clinical findings in patients with achromatopsia, macular degeneration, and other hereditary cone diseases. Hum Mutat 2005;25:248–58. [PubMed: 15712225]
28. Kohl S, Varsanyi B, Antunes GA, et al. CNGB3 mutations account for 50% of all cases with autosomal recessive achromatopsia. Eur J Hum Genet 2005;13:302–8. [PubMed: 15657609]
29. Kohl S, Baumann B, Broghammer M, et al. Mutations in the CNGB3 gene encoding the beta-subunit of the cone photoreceptor cGMP-gated channel are responsible for achromatopsia (ACHM3) linked to chromosome 8q21. Hum Mol Genet 2000;9:2107–16. [PubMed: 10958649]
30. Johnson S, Michaelides M, Aligianis IA, et al. Achromatopsia caused by novel mutations in both CNGA3 and CNGB3. J Med Genet 2004;41:e20. [PubMed: 14757870]
31. Sundin OH, Yang JM, Li Y, et al. Genetic basis of total colourblindness among the Pingelapese islanders. Nat Genet 2000;25:289–93. [PubMed: 10888875]

NIH-PA Author Manuscript

NIH-PA Author Manuscript

NIH-PA Author Manuscript

32. Kohl S, Baumann B, Rosenberg T, et al. Mutations in the cone photoreceptor G-protein alpha-subunit gene GNAT2 in patients with achromatopsia. Am J Hum Genet 2002;71:422–5. [PubMed: 12077706]
33. Aligianis IA, Forshew T, Johnson S, et al. Mapping of a novel locus for achromatopsia (ACHM4) to 1p and identification of a germline mutation in the alpha subunit of cone transducin (GNAT2). J Med Genet 2002;39:656–60. [PubMed: 12205108]
34. Nathans J, Maumenee IH, Zrenner E, et al. Genetic heterogeneity among blue-cone monochromats. Am J Hum Genet 1993;53:987–1000. [PubMed: 8213841]
35. Thaler ARG, Lessel MR, Heilig. Light induced oscillations of the standing potential in achromatopsia. Doc Ophthalmol 1986;63:333–336. [PubMed: 3492348]
36. Andreasson S, Tornqvist K. Electroretinograms in patients with achromatopsia. Acta Ophthalmol 1991;69:711–716. [PubMed: 1789084]
37. Crognale MA, Fry M, Highsmith J, et al. Characterization of a novel form of X-linked incomplete achromatopsia. Vis Neurosci 2004;21:197–203. [PubMed: 15518189]
38. Defoort-Dhellemmes S, Lebrun T, Arndt CF, et al. [Congenital achromatopsia: electroretinogram in early diagnosis]. J Fr Ophtalmol 2004;27:143–8. [PubMed: 15029041]
39. Michaelides M, Aligianis IA, Ainsworth JR, et al. Progressive cone dystrophy associated with mutation in CNGB3. Invest Ophthalmol Vis Sci 2004;45:1975–82. [PubMed: 15161866]
40. Wiesen MH, Sharpe LT, Zrenner E, Kohl S, Wissinger B, Jagle H. Rod function in patients with CNGA3 and CNGB3 mutations. Invest Ophthalmol Vis Sci. 2008ARVO E-Abstract 1267
41. Mayer DL, Hansen RM, Moore BD, Kim S, Fulton AB. Cycloplegic refractions in healthy children aged 1 through 48 months. Arch Ophthalmol 2001;119:1625–8. [PubMed: 11709012]
42. Zadnik K, Manny RE, Yu JA, et al. Ocular component data in schoolchildren as a function of age and gender. Optom Vis Sci 2003;80:226–36. [PubMed: 12637834]
43. Hansen, RM.; Fulton, AB. Development of scotopic retinal sensitivity. In: Simons, K., editor. Early Visual Development, Normal and Abnormal. New York: Oxford University Press; 1993. p. 130-142.
44. Fulton AB, Hansen RM. The development of scotopic sensitivity. Invest Ophthalmol Vis Sci 2000;41:1588–1596. [PubMed: 10798680]
45. Wongpichedchai S, Hansen RM, Koka B, Gudas VM, Fulton AB. Effects of halothane on children's electroretinograms. Ophthalmol 1992;99:1309–1312.
46. Fulton AB, Hansen RM, Moskowitz A. The cone electroretinogram in retinopathy of prematurity. Invest Ophthalmol Vis Sci 2008;49:814–9. [PubMed: 18235032]
47. Hansen RM, Fulton AB. Development of the cone ERG in infants. Invest Ophthalmol Vis Sci 2005;46:3458–62. [PubMed: 16123452]PMC1467576
48. Birch DG, Fish GE. Rod ERGs in retinitis pigmentosa and cone-rod degeneration. Invest Ophthalmol Vis Sci 1987;28:140–50. [PubMed: 3804644]
49. Hood DC, Birch DG. Rod phototransduction in retinitis pigmentosa: estimation and interpretation of parameters derived from the rod a-wave. Invest Ophthalmol Vis Sci 1994;35:2948–61. [PubMed: 8206712]
50. Lamb, TD.; Pugh, ENJ. Phototransduction in vertebrate rods and cones: Molecular mechanisms of amplification, recovery and light adaptation. In: Stavenga, DG.; deGrip, W.; Pugh, ENJ., editors. Handbook of Biological Physics. 3. Amsterdam: Elsevier; 2000. p. 183-255.
51. Lamb TD, Pugh EN Jr. A quantitative account of the activation steps involved in phototransduction in amphibian photoreceptors. J Physiol 1992;449:719–58. [PubMed: 1326052]
52. Pugh EN Jr, Lamb TD. Amplification and kinetics of the activation steps in phototransduction. Biochim Biophys Acta 1993;1141:111–49. [PubMed: 8382952]
53. Cideciyan AV, Jacobson SG. An alternative phototransduction model for human rod and cone ERG a-waves: normal parameters and variation with age. Vision Res 1996;36:2609–2621. [PubMed: 8917821]
54. Peachey NS, Alexander KR, Fishman GA. The luminance-response function of the dark-adapted human electroretinogram. Vision Res 1989;29:263–70. [PubMed: 2788958]
55. Granit R. The components of the retinal action potential in mammals and their relation to the discharge in the optic nerve. J Physiol 1933;77:207–239. [PubMed: 16994385]

NIH-PA Author Manuscript

NIH-PA Author Manuscript

NIH-PA Author Manuscript

56. Granit, R. Sensory Mechanisms of the Retina. London: Hafner Publishing Company; 1963. The components of the vertebrate electroretinogram; p. 38-68.
57. Aleman T, LaVail MM, Montemayor R, et al. Augmented rod bipolar cell function in partial receptor loss: an ERG study in P23H rhodopsin transgenic and aging normal rats. Vision Res 2001;41:2779–2797. [PubMed: 11587727]
58. Hood DC, Birch DG. A computational model of the amplitude and implicit time of the b-wave of the human ERG. Vis Neurosci 1992;8:107–126. [PubMed: 1558823]
59. Robson JG, Frishman LJ. Response linearity and kinetics of the cat retina: the bipolar cell component of the dark-adapted electroretinogram. Vis Neurosci 1995;12:837–50. [PubMed: 8924408]
60. Robson JG, Frishman LJ. Photoreceptor and bipolar cell contributions to the cat electroretinogram: A kinetic model for the early part of the flash response. J Opt Soc Am 1996;13:613–622.
61. Wurziger K, Lichtenberger T, Hanitzsch R. On-bipolar cells and depolarising third order neurons as the origin of the ERG b-wave in the RCS rat. Vision Res 2001;41:1091–1101. [PubMed: 11301082]
62. Akula JD, Mocko JA, Moskowitz A, Hansen RM, Fulton AB. The oscillatory potentials of the dark-adapted electroretinogram in retinopathy of prematurity. Invest Ophthalmol Vis Sci 2007;48:5788–5797. [PubMed: 18055833]
63. Marmor MF, Holder GE, Seeliger MW, Yamamoto S. Standard for clinical electroretinography (2004 update). Doc Ophthalmol 2004;108:107–14. [PubMed: 15455793]
64. Moskowitz A, Hansen R, Fulton A. Early ametropia and rod photoreceptor function in retinopathy of prematurity. Optom Vis Sci 2005;82:307–17. [PubMed: 15829858]
65. Cooper LL, Hansen RM, Darras BT, et al. Rod photoreceptor function in children with mitochondrial disorders. Arch Ophthalmol 2002;120:1055–1062. [PubMed: 12149059]
66. Carroll J, Choi SS, Williams DR. In vivo imaging of the photoreceptor mosaic of a rod monochromat. Vision Res. 2008 May 20;[Epub ahead of print]
67. Curcio CA, Sloan KR, Kalina RE, Hendrickson AE. Human photoreceptor topography. J Comp Neurol 1990;292:497–523. [PubMed: 2324310]
68. Hood, DC.; Birch, DG.; Birch, EE. Use of models to improve hypothesis delineation: A study of infant electroretinography. In: Simons, K., editor. Early Visual Development, Normal and Abnormal. New York: Oxford University Press; 1993. p. 517-535.
69. Chan TL, Martin PR, Clunas N, Grunert U. Bipolar cell diversity in the primate retina: morphologic and immunocytochemical analysis of a new world monkey, the marmoset Callithrix jacchus. J Comp Neurol 2001;437:219–39. [PubMed: 11494253]
70. Jones BW, Marc RE. Retinal remodeling during retinal degeneration. Exp Eye Res 2005;81:123–37. [PubMed: 15916760]
71. Jones BW, Watt CB, Marc RE. Retinal remodelling. Clin Exp Optom 2005;88:282–91. [PubMed: 16255687]
72. Marc RE, Jones BW. Retinal remodeling in inherited photoreceptor degenerations. Mol Neurobiol 2003;28:139–47. [PubMed: 14576452]
73. Lu M, Hansen RM, Cunningham MJ, Eklund SE, Fulton AB. Effects of desferoxamine on retinal and visual function. Arch Ophthalmol 2007;125:1581–2. [PubMed: 17998528]
74. Kolb H. The architecture of functional neural circuits in the vertebrate retina. The Proctor Lecture. Invest Ophthalmol Vis Sci 1994;35:2385–404. [PubMed: 8163331][erratum appears in Invest Ophthalmol Vis Sci1994;35:3576]
75. Raviola E, Gilula NB. Gap junctions between photoreceptor cells in the vertebrate retina. Proc Natl Acad Sci U S A 1973;70:1677–81. [PubMed: 4198274]
76. Nelson R. Cat cones have rod input: a comparison of the response properties of cones and horizontal cell bodies in the retina of the cat. J Comp Neurol 1977;172:109–35. [PubMed: 838876]
77. Smith RG, Freed MA, Sterling P. Microcircuitry of the dark-adapted cat retina: functional architecture of the rod-cone network. J Neurosci 1986;6:3505–17. [PubMed: 3794785]
78. Daw NW, Jensen RJ, Brunken WJ. Rod pathways in mammalian retinae. Trends Neurosci 1990;13:110–115. [PubMed: 1691871]
79. Schneeweis DM, Schnapf JL. Photovoltage of rods and cones in the macaque retina. Science 1995;268:1053–6. [PubMed: 7754386]

NIH-PA Author Manuscript

NIH-PA Author Manuscript

NIH-PA Author Manuscript

80. Sharpe LT, Stockman A. Rod pathways: the importance of seeing nothing. Trends Neurosci 1999;22:497–504. [PubMed: 10529817]
81. Buck, SL. Rod-cone interactions in human vision. In: Chapula, LM.; Werner, JS., editors. The Visual Neurosciences. Cambridge, MA: MIT Press; 2003. p. 863-878.
82. Haverkamp S, Michalakis S, Claes E, et al. Synaptic plasticity in CNGA3(−/−) mice: cone bipolar cells react on the missing cone input and form ectopic synapses with rods. J Neurosci 2006;26:5248–55. [PubMed: 16687517]
83. Wachtmeister L. Oscillatory potentials in the retina: What do they reveal. Prog Retin Eye Res 1998;17:485–521. [PubMed: 9777648]
84. Peachey NS, Alexander KR, Fishman GA. Rod and cone system contributions to oscillatory potentials: an explanation for the conditioning flash effect. Vision Res 1987;27:859–66. [PubMed: 3499028]
85. Kajiwara K, Berson EL, Dryja TP. Digenic retinitis pigmentosa due to mutations at the unlinked peripherin/RDS and ROM1 loci. Science 1994;264:1604–1608. [PubMed: 8202715]
86. Mohand-Said S, Hicks D, Leveillard T, Picaud S, Porto F, Sahel JA. Rod-cone interactions: developmental and clinical significance. Prog Retin Eye Res 2001;20:451–67. [PubMed: 11390256]
87. Ripps H. Cell death in retinitis pigmentosa: gap junctions and the 'bystander' effect. Exp Eye Res 2002;74:327–36. [PubMed: 12014914]
88. Pinilla I, Lund RD, Sauve Y. Contribution of rod and cone pathways to the dark-adapted electroretinogram (ERG) b-wave following retinal degeneration in RCS rats. Vision Res 2004;44:2467–74. [PubMed: 15358082]
89. Toda K, Bush RA, Humphries P, Sieving PA. The electroretinogram of the rhodopsin knockout mouse. Vis Neurosci 1999;16:391–8. [PubMed: 10367972]
90. Usukura J, Khoo W, Abe T, Breitman ML, Shinohara T. Cone cells fail to develop normally in transgenic mice showing ablation of rod photoreceptor cells. Cell Tissue Res 1994;275:79–90. [PubMed: 8118849]
91. Cideciyan AV, Hood DC, Huang Y, et al. Disease sequence from mutant rhodopsin allele to rod and cone photoreceptor degeneration in man. Proc Natl Acad Sci U S A 1998;95:7103–8. [PubMed: 9618546]
92. Chang B, Dacey MS, Hawes NL, et al. Cone photoreceptor function loss-3, a novel mouse model of achromatopsia due to a mutation in Gnat2. Invest Ophthalmol Vis Sci 2006;47:5017–21. [PubMed: 17065522]
93. Biel M, Seeliger M, Pfeifer A, et al. Selective loss of cone function in mice lacking the cyclic nucleotide-gated channel CNG3. Proc Natl Acad Sci U S A 1999;96:7553–7. [PubMed: 10377453]
94. Sidjanin DJ, Lowe JK, McElwee JL, et al. Canine CNGB3 mutations establish cone degeneration as orthologous to the human achromatopsia locus ACHM3. Hum Mol Genet 2002;11:1823–33. [PubMed: 12140185]
95. Komaromy AM, Alexander JJ, Cooper AE, et al. Targeting gene expression to cones with human cone opsin promoters in recombinant AAV. Gene Ther 2008;15:1073.
96. Alexander JJ, Umino Y, Everhart D, et al. Restoration of cone vision in a mouse model of achromatopsia. Nat Med 2007;13:685–7. [PubMed: 17515894]
97. Teller DY, McDonald MA, Preston K, Sebris SL, Dobson V. Assessment of visual acuity in infants and children: the acuity card procedure. Dev Med Child Neurol 1986;28:779–89. [PubMed: 3817317]

NIH-PA Author Manuscript
NIH-PA Author Manuscript
NIH-PA Author Manuscript

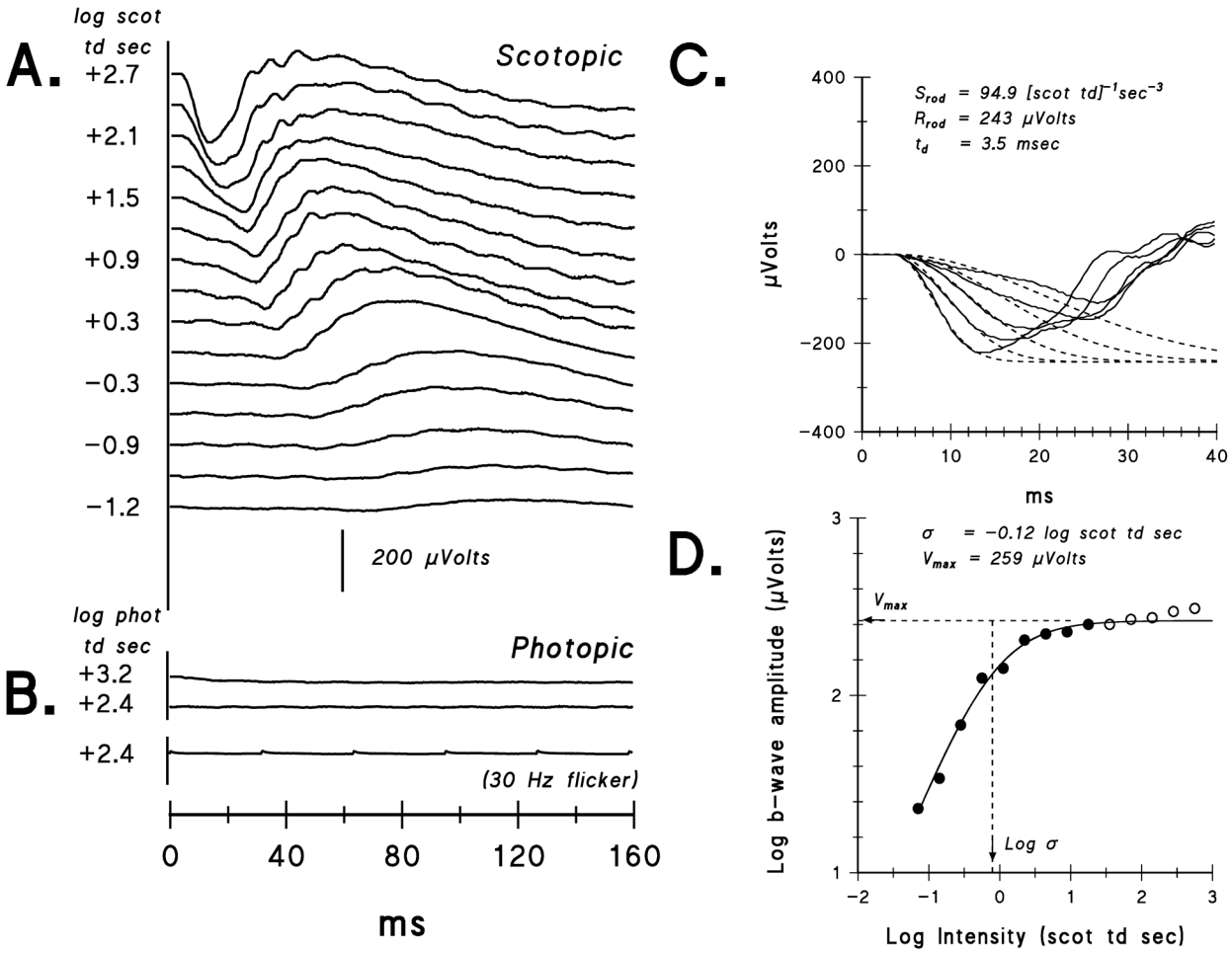

Figure 1.

Sample ERG results from an achromatopsia patient (ACHR #9) whose scotopic amplitudes are near the mean for patients. **A**. Dark-adapted ERG responses to a series of short wavelength flashes. For clarity, the stimulus intensity in log scot td sec is shown only for every other trace. **B**. Light-adapted ERG responses to two long wavelength flash intensities, +3.2 and +2.4 log phot td sec, and to 30 Hz flickering white light (+2.4 log phot td sec). The calibration bar pertains to panels **A** and **B. C**. The first 40 milliseconds of the ERG (solid lines) and the fit of Eq. 1 (dashed lines) to the leading edge of the a-wave. The parameters $\mathbf{S_{rod}}$ and $\mathbf{R_{rod}}$ for the model fit to the data are indicated. **D**. B-wave amplitude plotted as a function of stimulus intensity. Eq. 2 was fit up to ~+1.0 log scot td sec, indicated by the closed circles; parameters $\mathbf{V_{max}}$ and **log σ** are indicated.

NIH-PA Author Manuscript

NIH-PA Author Manuscript

NIH-PA Author Manuscript

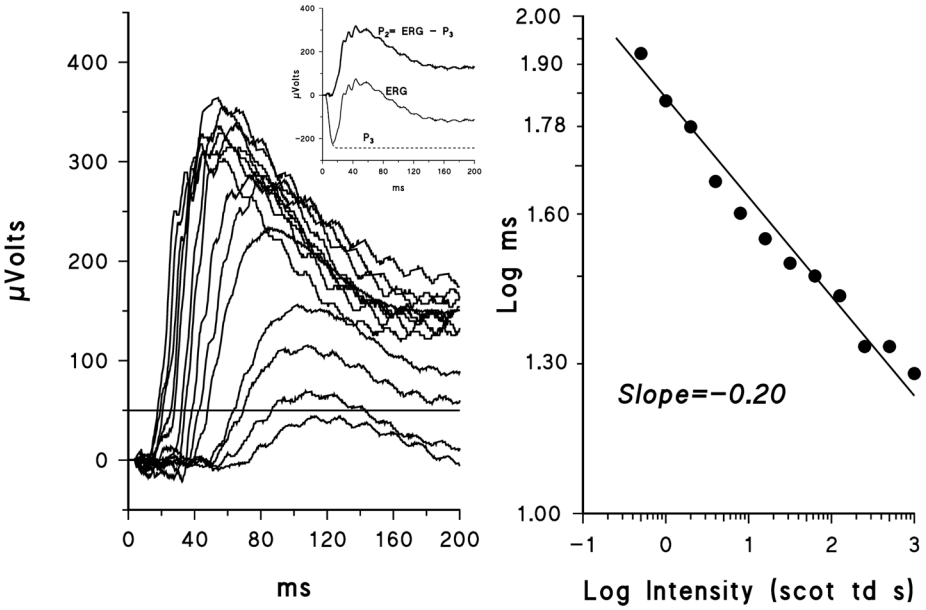

Figure 2.

A. Sample P_2 records from ACHR #9. The derivation of P_2 is shown in the inset. **B**. Latency at the 50 μVolt criterion plotted as a function of log stimulus intensity. The regression line has a slope of −0.20.

NIH-PA Author Manuscript
NIH-PA Author Manuscript
NIH-PA Author Manuscript

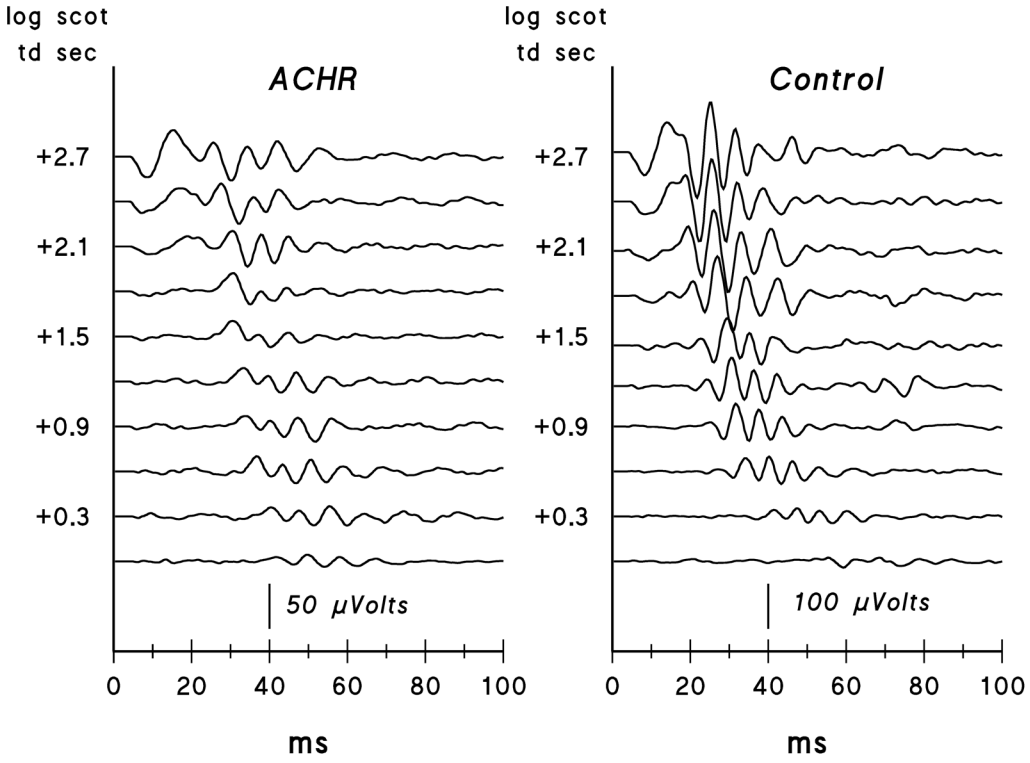

Figure 3.

Scotopic oscillatory potentials for a series of flash intensities from ACHR #9 (left) and for a control subject (right). For clarity, the stimulus intensity in log scot td sec is shown only for every other trace. Note that the achromatopsia patient's records are plotted at twice the gain of the control subject's.

NIH-PA Author Manuscript
NIH-PA Author Manuscript
NIH-PA Author Manuscript

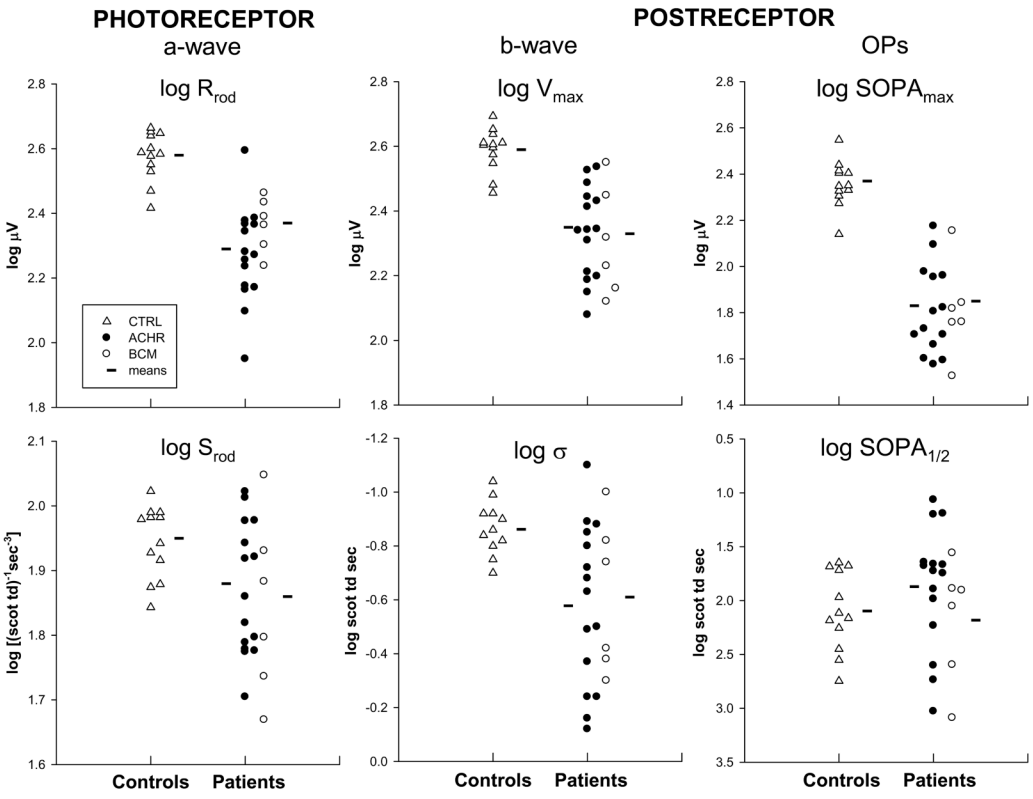

Figure 4.

Rod photoresponse parameters, $\mathbf{S_{rod}}$ and $\mathbf{R_{rod}}$, and postreceptor parameters, **log σ**, $\mathbf{V_{max}}$, **log** $\mathbf{SOPA_{1/2}}$, and $\mathbf{SOPA_{max}}$. Amplitude parameters ($\mathbf{R_{rod}}$, $\mathbf{V_{max}}$, and $\mathbf{SOPA_{max}}$) are shown on the top and sensitivity parameters ($\mathbf{S_{rod}}$, **log σ**, and **log** $\mathbf{SOPA_{1/2}}$) on the bottom. Log values are plotted for all parameters. Data for control subjects (triangles), patients with ACHR (filled circles), and BCM (open circles) are shown in each graph. The horizontal lines indicate the mean for each group.

NIH-PA Author Manuscript NIH-PA Author Manuscript NIH-PA Author Manuscript

Table 1

Characteristics of Achromatopsia and Blue Cone Monochromatism Patients

Patient No	Sex	Age at ERG (yr)	Spherical Equivalent (D)	Visual Acuity (most recent)	Photophobia	Nystagmus	PPR*
ACHR							
1	F	1.0	+3.75‡	20/190 §	Yes	Yes	Yes
2	F	1.1	+5.50‡	20/960 §	No	Yes	Yes
3	F	1.2	+6.50‡	20/250	Yes	Yes	No
4	M	1.5†	+7.75‡	20/500	Yes	Yes	No
5	M	1.6	+0.25	20/125	Yes	Yes	Yes
6	F	2.3	+4.00‡	20/133§	Yes	Yes	Yes
7	M	2.3	+8.50‡	20/180§	Yes	Yes	No
8	M	2.7	+2.00	20/400	Yes	Yes	Yes
9	F	3.0	+4.25‡	20/250	Yes	Yes	Yes
10	F	3.9	+8.00‡	20/300	Yes	Yes	Yes
11	F	4.9	−3.00‡	20/320	Yes	Yes	Yes
12	M	6.2†	+3.75‡	20/200	No	Yes	No
13	M	7.0	+1.00	20/222	Yes	Yes	Yes
14	M	7.7†	−4.75‡	20/200	Yes	Yes	No
15	F	20.2†	−1.50	20/125	Yes	Yes	Yes
BCM							
16	M	4.0	−2.88‡	20/160	Mild	Yes	Yes
17	M	6.8	−1.75‡	20/209	No	Yes	Yes
18	M	7.7	−6.13‡	20/400	Yes	Yes	Yes
19	M	8.3†	−1.63	20/160	Mild	Yes	No
20	M	9.4†	−0.50	20/80	Mild	Yes	Yes
21	M	22.1†	−10.25‡	20/130	Mild	Yes	No

*PPR: paradoxical pupillary response

†tested awake

‡outside 99% prediction limit for normal[41, 42]

§grating acuity (Teller Acuity Cards)[97]